Superconductivity of barium-VI synthesized via compression at low temperatures

D. E. Jackson,[1] D. VanGennep,[1] Y. K. Vohra,[2] S. T. Weir,[3] and J. J. Hamlin[1,*]
[1]*Department of Physics, University of Florida, Gainesville, Florida 32611, USA*
[2]*Department of Physics, University of Alabama at Birmingham, Birmingham, Alabama 35294, USA*
[3]*Physics Division, Lawrence Livermore National Laboratory, Livermore, California 94550, USA*
(Received 18 July 2017; revised manuscript received 30 October 2017; published 15 November 2017)

Using a membrane-driven diamond anvil cell and both ac magnetic susceptibility and electrical resistivity measurements, we have characterized the superconducting phase diagram of elemental barium to pressures as high as 65 GPa. We have determined the superconducting properties of the recently discovered Ba-VI crystal structure, which can only be accessed via the application of pressure at low temperature. We find that Ba-VI exhibits a maximum T_c near 8 K, which is substantially higher than the maximum T_c found when pressure is applied at room temperature. We discuss our results in terms of the implications for pressure-induced superconductivity in other elements exhibiting complex/modulated structures at high pressure. Finally, we highlight the potential of cryogenic compression to reveal additional richness in previously explored high-pressure phase diagrams.

DOI: 10.1103/PhysRevB.96.184514

I. INTRODUCTION

Experiments under applied high pressures have played an important role in advancing our understanding of relationships between crystal structures and superconducting properties [1,2]. It is well known that the critical pressures for structural transitions are sometimes strongly temperature dependent [3] and therefore one must use caution when comparing room-temperature structural information to trends in (usually low-temperature) superconducting critical temperatures [4]. Furthermore, in some cases, the thermodynamic history of the sample can strongly influence superconducting [5] and/or structural [6] properties. For example, if there is a kinetic barrier for the transition to the stable phase, applying or releasing pressure at low temperatures can lead to a crystal structure persisting far outside of the range of pressures for which it is thermodynamically stable [7]. An arguably more dramatic manifestation of such effects can occur if a barrier for the transition to the stable phase causes an entirely new metastable crystal structure to emerge. This was recently found for elemental Ba metal, with the observation of a new metastable structural phase (Ba-VI) that only appears when pressure is applied at temperatures below ∼100 K [8]. In this paper, we have determined the superconducting properties of this newly discovered phase of Ba. The superconducting properties of the alkaline-earth metals elements (Be, Mg, Ca, Sr, Ba, Ra) are of particular interest because Ca at high pressure exhibits the highest superconducting critical temperature of any of the elemental solids with $T_c \sim 21$–29 K at pressures above 200 GPa [9–12].

The room-temperature crystal structures of Ba at high pressure have been studied to pressures as high as 110 GPa [13–15]. These studies revealed structural phase transitions from Ba-I (bcc) at ambient pressure to Ba-II (hcp), Ba-IV, and Ba-V (hcp) at pressures of 5, 12, and 45 GPa, respectively. Early reports of a Ba-"III" phase, existing between Ba-II and Ba-IV, appear to have been refuted, though a new phase, also labeled Ba-III, may form in a very narrow temperature and pressure range (∼5–7 GPa at ∼700–800 K) [15]. Ba-IV in particular has received a great deal of attention because of its extremely complex modulated "host-guest" structures, comprising coexisting interpenetrating sublattices [16]. The label "Ba-IV" actually refers to a series of closely related structures (Ba-IVa through Ba-IVd) built upon the same host-guest structural motif. It is within the pressure range that Ba-IV exists that Ba exhibits a maximum T_c value of ∼5 K at 18 GPa.

When Ba is compressed at temperatures below ∼100 K, a substantial energy barrier inhibits the Ba(II → IV) transition and instead a new structure, denoted Ba-VI, appears [8]. Unlike complex Ba-IV, Ba-VI adopts a rather simple orthorhombic structure. The Ba-VI structure exists for pressures in the range of 12–30 GPa at low temperature, and the structure appears to be metastable, as evinced by the fact that on warming above ∼100 K it transforms to Ba-IV. Figure 1(a) schematically represents the structural phase diagram reported in Ref. [8].

We emphasize that Desgreniers *et al.* [8] found that Ba-VI cannot be synthesized by cooling from Ba-IV. Previous studies of the superconducting properties of Ba have nearly all been carried out by applying pressure at room temperature, and then cooling at constant pressure, so that the most widely reported and quoted T_c values correspond to Ba-IV rather than Ba-VI [17–19]. There are two exceptions. In the 1972 report of Il'ina *et al.* [20], pressures up to 19 GPa were applied at 4.2 K, resulting in critical temperatures about 0.5 K lower than found for room-temperature pressure application. In 1989, Bireckoven and Wittig [21,22] described an experiment in which they released pressure from 50 GPa at low temperatures. They found that below 35 GPa, T_c began to increase more rapidly, eventually reaching up to 7 K at 27 GPa. They attributed the higher critical temperature to the metastability of Ba-V on pressure release. However, with the new structural information [8], one may wonder if perhaps the increase in T_c was due to the formation of Ba-VI.

In the present study, we have performed measurements up to ∼65 GPa using a membrane-driven diamond anvil cell which allows pressure changes at low temperature. In order to unmask the superconducting properties of Ba-VI we have used a combination of ac magnetic susceptibility (ACS) measurements, which are sensitive to the superconductivity of the bulk phase, and electrical resistivity measurements, which are sensitive the superconductivity of small amounts

*Corresponding author: jhamlin@ufl.edu

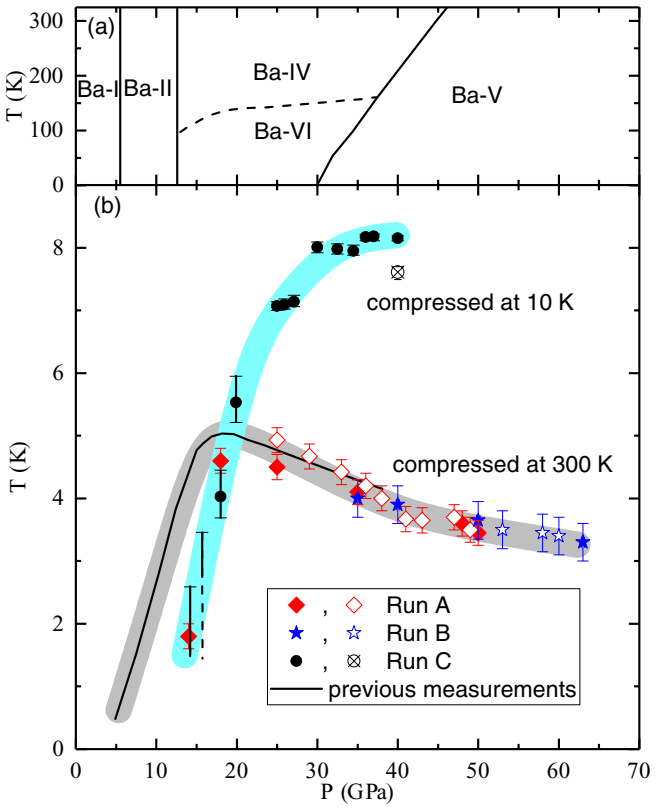

FIG. 1. (a) Schematic structural phase diagram for Ba based on Ref. [8]. (b) Phase diagram indicating superconducting critical temperature vs pressure. The solid black line indicates T_c as determined by previous measurements in which pressure was varied at room temperature [17–19]. The T_c of Ba-VI (black circles) reaches substantially higher values than any of the other structures of Ba. Further details of each measurement run are summarized in Table I.

of minority phase. We find that Ba-VI exhibits a maximum T_c near 8 K, which is significantly higher that the highest value reported for Ba-IV (5 K). We have also performed ACS measurements of the pressure dependence of T_c for Ba-V in the vicinity of the Ba(V $\rightarrow$ VI) transition by unloading pressure at low temperature. We find no evidence for the substantial T_c enhancement in metastable Ba-V suggested by Bireckoven and Wittig [21,22]. Together with Ba, a number of other elements exhibit complex crystal structures with commensurate or incommensurate modulations at high pressure [23], and we discuss what our results might imply for the superconducting phase diagrams of such systems.

II. METHODS

Pieces of Ba with typical dimensions around 100 μm $\times$ 100 μm $\times$ 10 μm were cut from a large piece of 5N purity Ba. The sample was cut and loaded into the diamond anvil cell inside of a nitrogen-filled purified glove box. The measurements were made in an OmniDAC gas membrane-driven diamond anvil cell from Almax-EasyLab. The cell was placed inside a custom continuous-flow cryostat built by Oxford Instruments. A fiber entering the top of the cryostat via a feedthrough and windows on the bottom of the cryostat provide optical access to the cell. The pressure was determined using either the fluorescence of the R_1 peak of small ruby chips placed next to the sample [24] or from the Raman signal from the anvil [25]. The gas membrane and optical access allows us to change and measure pressure *in situ* at low temperatures.

TABLE I. Summary of the different sets of measurements. The symbols in the leftmost column correspond to the symbols used in the phase diagram presented in Fig. 1. The column labeled "Type" indicates whether resistivity (ρ) or ac magnetic susceptibility (χ) was measured. "Measurement sequence" indicates the path that was taken through temperature-pressure phase space.

Run	Type	Measurement sequence
Run A (◆, ◇)	χ	Measurements up to ~49 GPa performed while applying pressure at room temperature (solid diamond). Unloading measurements performed while maintaining $T \lesssim 10$ K (open diamond).
Run B (★, ☆)	χ	Measurements up to ~63 GPa performed while applying pressure at room temperature (solid star). Unloading measurements performed while maintaining $T \lesssim 10$ K (open star).
Run C (●, ⊗)	ρ	Pressure increased to 8 GPa at room temperature and then cooled. Further measurements performed during pressure application below 10 K (solid circle). At the highest pressure, the sample was "annealed" at 50 K for 3 h before remeasuring at the same pressure (circle with cross).

Resistivity was measured by using a designer diamond anvil with eight symmetrically positioned, deposited tungsten microprobes encapsulated in high-quality homoepitaxial diamond [26]. This diamond had a flat of approximately 180 μm. Solid steatite was used as the pressure medium. Resistance was measured in a four-probe arrangement using Keithley 6221 and Keithley 2182a configured for the "delta mode." From the resistance, R we estimated the sample resistivity using the van der Pauw equation $\rho = (\pi t R / \ln 2)$, where t is the estimated thickness of the sample [27]. Given the uncertainty in the sample thickness, the estimated resistivity is accurate to within about a factor of 2. We have not attempted to account for the effect of changes in the sample thickness with pressure on the resistivity estimate.

The ac magnetic susceptibility measurements were performed using a balanced primary/secondary coil system [28]. Daphne oil was used as the pressure medium for the ACS experiments. The primary provides a root mean square field of ~3 G at 1000 Hz. The coils are connected to two Stanford Research SRS830 lock-in amplifiers measuring at both the first and the third harmonic of the excitation frequency [29]. The detection coil is connected through a Stanford Research SR554 transformer/preamplifier. The third harmonic measurement is useful because it is less affected by background changes unrelated to the superconducting transition than the first harmonic signal. Several different resistivity or ACS experiments were performed while taking different paths through the pressure-temperature phase space. Table I summarizes the different experiments that were performed.

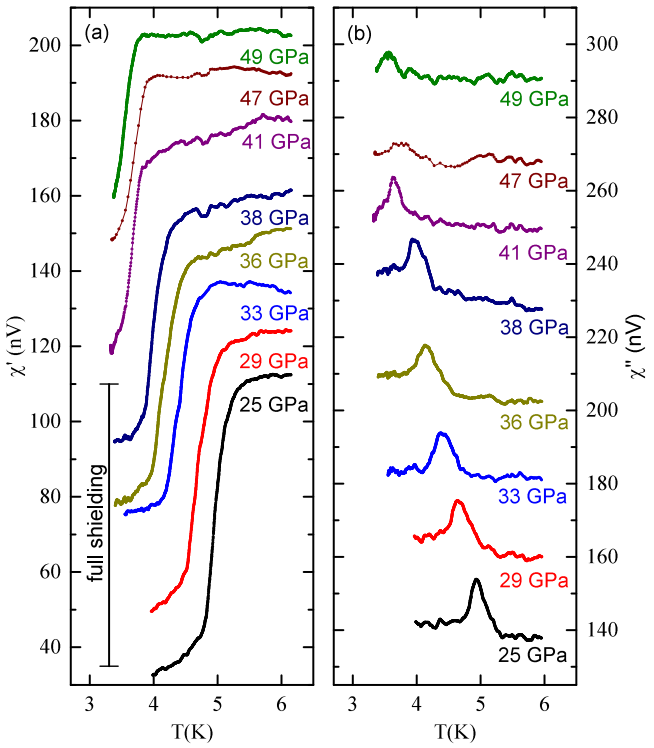

FIG. 2. (a) Real and (b) imaginary parts of the magnetic susceptibility for run A while unloading the pressure below 10 K. Each curve has been offset by a constant value for clarity. The sizes of the transitions are consistent with the estimated jump for a full shielding indicated by the scale bar at the bottom left of the figure.

III. RESULTS

A phase diagram summarizing our results is presented in Fig. 1(b). Runs A and B were aimed primarily at clarifying the superconducting properties of Ba-V. In these experiments, pressure was increased at room temperature to pressures above 45 GPa, where the Ba(IV $\rightarrow$ V) transition occurs. For both set of measurements, during loading, the sample was cooled to low temperature several times and T_c was measured. Once the maximum pressure was reached, the sample was annealed at room temperature for at least 6 h before cooling in order to help ensure complete transformation of the sample to Ba-V. The sample was then cooled to low temperature and maintained below $\sim$10 K while subsequent measurements of T_c were taken during unloading.

Figure 2 presents a representative sample of our magnetic susceptibility data from run A. The data shown correspond to measurements taken while unloading pressure at low temperature. Superconducting transitions are clearly visible both as drops in the real part of the susceptibility (χ') and peaks in the imaginary part of the susceptibility (χ''). From the geometry of the coil system, the approximate size and shape of the sample, and the calculated demagnetization factor for the sample [30], we arrive at an estimate that full shielding should give a transition of about 75 nV in χ'. Our susceptibility data are thus consistent with bulk superconductivity. The T_c values plotted in Fig. 1(b) have been taken from the midpoint of the χ' transition, and the error bar represents the 20%–80% transition width.

The susceptibility data from runs A and B show that T_c varies smoothly with pressure across the Ba(IV $\rightarrow$ V) transition with no discernible change in the slope dT_c/dP. In run A, we reduced the pressure to 25 GPa at low temperature, which is lower that the critical pressure for the Ba(V $\rightarrow$ VI) transition (30 GPa), yet we found that T_c versus pressure agreed closely with the data obtained during room-temperature loading [31]. The similarity of the room-temperature loading and low-temperature unloading curves across the Ba(V $\rightarrow$ VI) transition suggests that either (1) Ba-IV, Ba-V, and Ba-VI all have nearly the same T_c in the vicinity of 30 GPa, or (2) on unloading at low temperature the Ba(V $\rightarrow$ VI) transition does not occur immediately so that the sample remains in the Ba-VI structure to pressures below 30 GPa. We note that Desgreniers *et al.* [8] did not seem to explore whether there is any hysteresis in the Ba(V $\rightarrow$ VI) transition. Below, we will see that run C suggests that the latter of the two above possibilities is probably correct.

In run C, we measured electrical resistivity and approached the Ba-VI structure from the low-pressure side. An initial pressure of $\sim$8 GPa was applied at room temperature and then the sample was cooled to low temperature. At this point the sample is expected to be the Ba-II structure. Subsequent pressure increases were carried out while the temperature was kept below 10 K, which should drive the sample across the Ba(II $\rightarrow$ VI) transition. Figure 3(a) shows the electrical resistivity versus temperature for several different pressures. At 10 and 11 GPa we observed no trace of superconductivity down to $\sim$3 K. Broad, incomplete superconducting transitions first appear at 14 GPa and the transitions become complete (reaching effectively zero resistance) for pressures at and above 18 GPa. The transition remains broad to 20 GPa and then suddenly becomes much sharper at higher pressures. Remarkably, we find that T_c increases to $\sim$8 K by 30 GPa, which is about 60% higher than the highest T_c observed in previous measurements in which pressure was applied at room temperature.

Above 30 GPa, which is the critical pressure for the Ba(VI $\rightarrow$ V) transition, T_c saturates at 8 K and remains roughly constant up to 40 GPa. The fact that T_c does not immediately drop to the values expected for Ba-V (4–5 K) at pressures above 30 GPa suggest that the Ba(VI $\rightarrow$ V) transition is sluggish at these low temperatures. We note that since T_c was measured via resistivity, it is possible that part of the sample has converted to Ba-V, while enough Ba-VI remains to allow a supercurrent to percolate through the sample. This scenario is supported by the lower panel of Fig. 3, which shows the resistivity versus pressure measured at 10 K. The resistivity increases sharply with pressure in the Ba-VI region. At 30–34 GPa the resistivity appears to saturate. At still higher pressures the resistivity begins to drop. At 40 GPa, we raised the temperature to 50 K and annealed the sample for 3 h before cooling back down to remeasure. After this annealing process, the resistivity dropped sharply by a factor of 2 [crossed circle in Fig. 3(b)], and the superconducting transition dropped by about half a kelvin and became substantially broader. These observations support the conclusion that the pressure-driven Ba(VI $\rightarrow$ V) transition is not immediate when the sample is maintained at low temperatures.

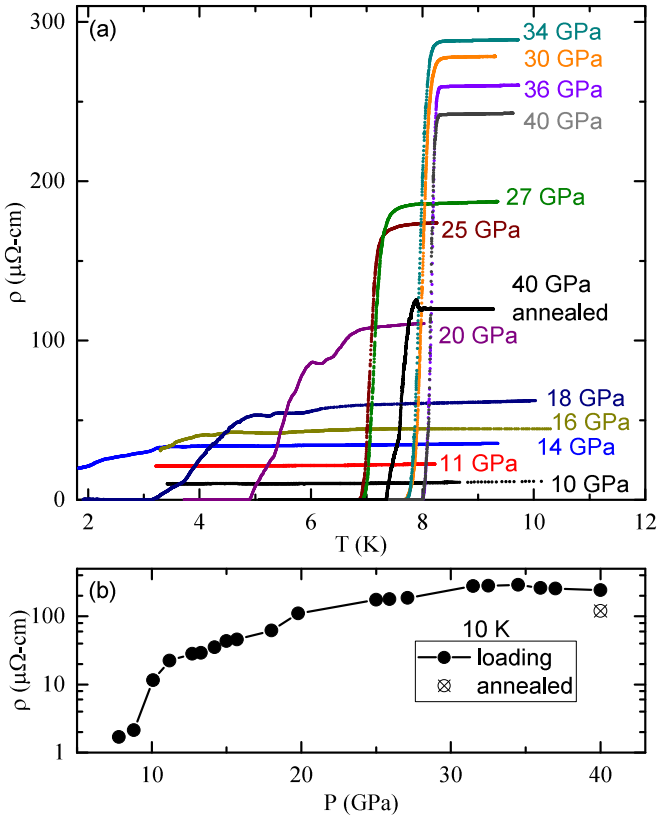

FIG. 3. (a) Run C resistivity data taken while increasing the pressure at 10 K so as to enter the Ba-VI state. Superconductivity was observed beginning at 14 GPa with an incomplete transition above 2 K. The critical temperature peaked slightly above 8 K at 30 GPa. At 40 GPa, the sample was annealed for 3 h at 50 K, resulting in a slight drop in T_c and broadening of the transition. (b) Resistivity at 10 K vs pressure for run C. The resistivity dropped by factor of ∼2 after annealing at 50 K. The changes in the magnitude of the resistivity and superconducting transition after annealing suggest that the sample has partially converted to Ba-V.

IV. DISCUSSION

Using first-principles calculations, Desgreniers *et al.* estimated $T_c = 3.6$ K at 16.2 GPa for the Ba-VI structure. This value matches our results quite well—we found a resistive onset temperature of about 3.5 K at 16.5 GPa. It does not seem that these calculations have been carried out at different pressures within the Ba-VI structure, and it would be interesting to see if theory reproduces the positive dT_c/dP trend that we have observed here. Another theoretical effort addressed the Ba-V structure and computed values of T_c ranging from 7.8 to 9.5 K at 45 GPa [32]. This is somewhat higher than the $T_c \sim 3.5$ K that we have observed at this pressure, however, the slope dT_c/dP they compute (∼0.1 K/GPa) is roughly equal to what we find for the Ba-V in the pressure range 30–65 GPa. The complexity of the Ba-IV crystal structure apparently makes first-principles superconducting parameter computation intractable without the use of structural approximations.

Trends in the superconducting and structural behavior of the alkaline-earth metals, as well as many other elements, can be understood in terms of the pressure-induced transfer of *sp* electrons into *d* states [2]. At ambient pressure, Be is marginally superconducting with a T_c of only 26 mK, and none of the other alkaline-earth metals are superconducting. Under high pressure, the light alkaline-earth-metal elements (Be and Mg) do not show any enhancement of superconductivity, while the heavy alkaline-earth metals (Ca, Sr, and Ba) all become superconducting. This difference in behavior derives from the fact that Be and Mg have no nearby *d* states, while Ca, Sr, and Ba do. As pressure increases, the *s* electrons in Ca, Sr, and Ba transfer into *d* bands so that these elements become transition-metal-like at high pressure. The substantial density of states at the Fermi level due to these *d* states is favorable for superconductivity. Across the heavy alkaline-earth metals, superconductivity only seems to appear when the number of *d* electrons N_d exceeds ∼0.92 [33]. In addition, the appearance of complex modulated structures in the alkaline-earth metals has been connected with the near completion $s \rightarrow d$ transfer [16]. The completion of $s \rightarrow d$ transfer, the onset of superconductivity, and the appearance of modulated structures all occur at progressively higher pressures going from Ba, to Sr, to Ca [2]. Barium at lower pressures can thus be considered as a close analog of Sr and Ca at higher pressures.

The present results show that a significant T_c enhancement can be obtained by avoiding the complex modulated Ba-IV structure. Why might this be, and what does this imply for the superconducting phase diagrams of Ca, Sr, and other elements exhibiting pressure-induced complex modulated crystal structures? The modulated structures that appear in several elements have been attributed to the formation of a charge density wave (CDW) [34–36]. A synonymous interpretation views these structures as deriving from Fermi-surface/Brillouin-zone interactions that lead to the opening of pseudogap at the Fermi level [37–39]. Both CDW/pseudogap states and superconductivity rely on a modification of the density of states at the Fermi level, and this can result in a competition between the two phases such that suppressing the CDW/pseudogap leads to an enhancement of T_c [40]. Among the elemental solids, S is one of the prototypes for this behavior: The increase of T_c in the complex S-IV structure has been related the suppression and then destruction of a CDW [34,41]. In the case of U, the suppression of several CDW transitions correlates with a maximum in the T_c vs pressure curve [23,42,43]. For P, calculations involving a commensurate approximation of the incommensurate P-IV structure indicate a suppression of T_c in the modulated structure compared to nearby simple cubic and simple hexagonal structures [44]. The T_c suppression was attributed to a lowering of the density of states due to the modulation. A similar scenario may be at play for Ba such that the T_c of Ba-IV is suppressed due to the presence of a pseudogap. On the other hand, Loa *et al.* [16] performed electronic structure calculations for a simplified approximation of the Ba-IVc structure and found no indication of a pseudogap. Furthermore, it is possible that the higher T_c of Ba-VI relative to Ba-IV derives from gross differences in the crystal structures, rather than the presence of a pseudogap in Ba-IV. Low-temperature compression (and decompression) experiments in elements including P [45] and Si [46] have revealed T_c enhancements that are likely unrelated to the type of CDW/superconductivity competition described above.

Nonetheless, the present results and the above factors hint that other elements crystallizing in complex modulated structures at room temperature might exhibit enhanced superconducting critical temperatures when compressed at low temperature. Desgreniers *et al.* [8] proposed that systems exhibiting complex modulated structures structures at ambient temperatures may show a general tendency to adopt alternative metastable structures when pressurized cryogenically. The kinetics of solid-solid phase transitions are still incompletely understood [47] so that it is an open question whether or not such metastable structures will appear in any particular case.

It is interesting to consider whether metastable structures might show a general bias towards superconductivity. The existence of a small energy barrier to a more stable structure implies the presence of an ion in a shallow potential well. A shallow well will produce a low-frequency phonon mode. Owing to the $1/\omega$ in the Eliashberg integral for the electron-phonon coupling $\lambda = 2\int_0^\infty d\omega\, \alpha^2 F(\omega)/\omega$, a low-frequency mode contributes to a large λ. Provided that λ is large enough to overcome the average Coulomb repulsion μ^*, T_c can be nonzero. Hence metastable phases ought to tend towards exhibiting superconductivity. On the other hand, a small ω will contribute to a low prefactor in, e.g., the McMilllan equation [48],

$$T_c = \frac{\langle\omega\rangle}{1.20} \exp\left[\frac{-1.04(1+\lambda)}{\lambda - \mu^*(1+0.62\lambda)}\right], \quad (1)$$

which can lead to lower values of the critical temperature. Of course, additional complexities could cause this simple picture to break down in any given material.

V. CONCLUSIONS

Experiments aimed at probing the effects of low-temperature compression on both the structural and superconducting properties of elements with incommensurate/modulated structures may offer a different perspective on the occurrence of superconductivity throughout the periodic table. Given the closely similar superconducting/structural phase diagrams of the heavy alkaline-earth metals, low-temperature compression experiments are particularly well motivated for Ca, which exhibits the highest critical temperature among the elements ($T_c > 21$ K) in a host-guest structure at pressures above 210 GPa [11]. The majority of high-pressure experiments to date have been carried out by applying pressure at room temperature, and further cryogenic compression experiments promise to reveal additional richness in the phase diagrams of many materials.

ACKNOWLEDGMENTS

The development of *in situ* pressure tuning equipment was partially supported by The National High Magnetic Field Laboratory User Collaboration Grants Program. The National High Magnetic Field Laboratory is supported by National Science Foundation Cooperative Agreement No. DMR-1157490 and the State of Florida. Measurements were supported by NSF Grant No. DMR-1453752. Designer diamond anvils were supported by DOE-NNSA Grant No. DE-NA0002928 and under the auspices of the U.S. Department of Energy by Lawrence Livermore National Laboratory under Contract No. DE-AC52-07NA27344. We thank A. Linscheid for helpful conversations.

[1] J. S. Schilling, in *Frontiers of High Pressure Research II: Application of High Pressure to Low-Dimensional Novel Electronic Materials* (Springer, Berlin, 2001), pp. 345–360.
[2] J. J. Hamlin, Physica C **514**, 59 (2015).
[3] J. Cannon, J. Phys. Chem. Ref. Data **3**, 781 (1974).
[4] T. Matsuoka, M. Sakata, Y. Nakamoto, K. Takahama, K. Ichimaru, K. Mukai, K. Ohta, N. Hirao, Y. Ohishi, and K. Shimizu, Phys. Rev. B **89**, 144103 (2014).
[5] S. Sadewasser, Y. Wang, J. S. Schilling, H. Zheng, A. P. Paulikas, and B. W. Veal, Phys. Rev. B **56**, 14168 (1997).
[6] G. J. Ackland, M. Dunuwille, M. Martinez-Canales, I. Loa, R. Zhang, S. Sinogeikin, W. Cai, and S. Deemyad, Science **356**, 1254 (2017).
[7] M. I. Eremets, R. J. Hemley, H.-k. Mao, and E. Gregoryanz, Nature (London) **411**, 170 (2001).
[8] S. Desgreniers, J. S. Tse, T. Matsuoka, Y. Ohishi, Q. Li, and Y. Ma, Appl. Phys. Lett. **107**, 221908 (2015).
[9] S. Okada, K. Shimizu, T. Kobayashi, K. Amaya, and S. Endo, J. Phys. Soc. Jpn. **65**, 1924 (1996).
[10] T. Yabuuchi, T. Matsuoka, Y. Nakamoto, and K. Shimizu, J. Phys. Soc. Jpn. **75**, 083703 (2006).
[11] M. Sakata, Y. Nakamoto, K. Shimizu, T. Matsuoka, and Y. Ohishi, Phys. Rev. B **83**, 220512 (2011).
[12] M. Andersson, Phys. Rev. B **84**, 216501 (2011).
[13] T. Kenichi, Phys. Rev. B **50**, 16238 (1994).
[14] W. Winzenick and W. Holzapfel, in *High Pressure Science and Technology*, edited by W. Trzeciakowski (World Scientific, Singapore, 1996), pp. 384–386.
[15] M. Winzenick and W. B. Holzapfel, Phys. Rev. B **55**, 101 (1997).
[16] I. Loa, R. J. Nelmes, L. F. Lundegaard, and M. I. McMahon, Nat. Mater. **11**, 627 (2012).
[17] J. Wittig and B. T. Matthias, Phys. Rev. Lett. **22**, 634 (1969).
[18] A. R. Moodenbaugh and J. Wittig, J. Low Temp. Phys. **10**, 203 (1973).
[19] K. J. Dunn and F. P. Bundy, Phys. Rev. B **25**, 194 (1982).
[20] M. A. Il'ina, E. S. Itskevich, and E. M. Dizhur, Sov. Phys. JETP **34**, 1263 (1972).
[21] B. Bireckoven and J. Wittig, in *Proceedings of the 11 International Conference AIRAPT*, High-Pressure Science and Technology Vol. 3 (Naukova Dumka, Kiev, 1989), pp. 14–24.
[22] E. Y. Tonkov, *High Pressure Phase Transformations Handbook 3* (Gordon and Breach, Philadelphia, 1996).
[23] M. I. McMahon and R. J. Nelmes, Chem. Soc. Rev. **35**, 943 (2006).
[24] G. J. Piermarini, S. Block, J. D. Barnett, and R. A. Forman, J. Appl. Phys. **46**, 2774 (1975).
[25] M. Hanfland and K. Syassen, J. Appl. Phys. **57**, 2752 (1985).
[26] S. T. Weir, J. Akella, C. Aracne-Ruddle, Y. K. Vohra, and S. A. Catledge, Appl. Phys. Lett. **77**, 3400 (2000).

[27] X. Huang, C. Gao, Y. Han, M. Li, C. He, A. Hao, D. Zhang, C. Yui, G. Zou, and Y. Ma, Appl. Phys. Lett. **90**, 242102 (2007).
[28] S. Deemyad, J. S. Schilling, J. D. Jorgensen, and D. G. Hinks, Physica C **361**, 227 (2001).
[29] T. Ishida and R. B. Goldfarb, Phys. Rev. B **41**, 8937 (1990).
[30] A. Aharoni, J. Appl. Phys. **83**, 3432 (1998).
[31] The first data point obtained on loading for run A ($P \sim 14$ GPa, $T_c \sim 1.8$ K) should correspond to the Ba-VI structure. For this particular measurement, a pressure of 9 GPa was applied at room temperature. During cooling, the pressure increased to 14 GPa. The pressure exceeded 12.5 GPa at about 70 K. This path will produce the metastable Ba-VI structure rather than Ba-IV.
[32] D. Zhou, C.-Y. Pu, H.-Z. Song, G.-Q. Li, J.-F. Song, L. Cheng, and B. Gang, Chin. Phys. B **22**, 087403 (2013).
[33] H. L. Skriver, Phys. Rev. Lett. **49**, 1768 (1982).
[34] O. Degtyareva, M. V. Magnitskaya, J. Kohanoff, G. Profeta, S. Scandolo, M. Hanfland, M. I. McMahon, and E. Gregoryanz, Phys. Rev. Lett. **99**, 155505 (2007).
[35] I. Loa, M. I. McMahon, and A. Bosak, Phys. Rev. Lett. **102**, 035501 (2009).
[36] H. Nagara, K. Mukose, T. Ishikawa, M. Geshi, and N. Suzuki, J. Phys.: Conf. Ser. **215**, 012107 (2010).
[37] V. F. Degtyareva, High Press. Res. **23**, 253 (2003).
[38] G. J. Ackland and I. R. Macleod, New J. Phys. **6**, 138 (2004).
[39] V. Degtyareva, Phys. Usp. **49**, 369 (2006).
[40] G. Bilbro and W. McMillan, Phys. Rev. B **14**, 1887 (1976).
[41] M. Monni, F. Bernardini, A. Sanna, G. Profeta, and S. Massidda, Phys. Rev. B **95**, 064516 (2017).
[42] M. B. Maple and D. Wohlleben, Phys. Lett. **38**, 351 (1972).
[43] G. Lander, E. Fisher, and S. Bader, Adv. Phys. **43**, 1 (1994).
[44] A. Nakanishi, T. Ishikawa, H. Nagara, K. Shimizu, and H. Katayama-Yoshida, High Press. Res. **32**, 3 (2012).
[45] H. Kawamura, I. Shirotani, and K. Tachikawa, Solid State Commun. **54**, 775 (1985).
[46] T. Valyanskaya and G. Stepanov, Solid State Commun. **86**, 723 (1993).
[47] S. Pogatscher, D. Leutenegger, P. J. Uggowitzer, and J. F. Lo, Nat. Commun. **7**, 11113 (2016).
[48] R. Dynes, Solid State Commun. **10**, 615 (1972).